# Cumulative Ionization in Optically Pumped Helium Discharges: A Source of Polarized Electrons*

M. V. McCusker,† L. L. Hatfield,‡ and G. K. Walters
*Rice University, Houston, Texas* 77001
(Received 21 June 1971)

Polarization analysis of electrons extracted from a weak helium discharge in which the $2\,^3S_1$ metastable atoms are spin oriented by optical pumping indicates that the reaction $He(2\,^3S_1) + He(2\,^3S_1) \rightarrow He(1\,^1S_0) + He^+ + e^-$ is the predominant source of ionization in the discharge. The reaction conserves spin angular momentum and therefore produces polarized electrons. The process has been exploited to produce continuous beams of electrons with polarization as high as 10%. For a source-gas pressure of 0.035 torr, a continuous 4-$\mu$A beam with 8% spin polarization has been realized. Electrons extracted from the late afterglow of a pulsed discharge have 17% polarization at an optimum pressure of 0.1 torr.

## I. INTRODUCTION

In the past there have been several studies, both theoretical and experimental, which have attempted to determine the specific ionization mechanisms that occur in a helium discharge.[1] These studies have indicated that cumulative or multiple-step ionization processes probably play a significant role in maintaining both dc and high-frequency discharges; however, the importance of cumulative ionization in such discharges has never been directly tested by experiment. In this paper we present direct evidence of the importance of ionization processes involving the metastable $2\,^3S_1$ state in helium; we also demonstrate that under certain conditions the only ionization processes that produce electrons at a rate sufficient to maintain the discharge are cumulative. Moreover, as a result of carrying out this investigation, we have developed a method of producing an intense beam of polarized electrons suitable for use in electron scattering experiments.[2]

In helium the first excited state $2\,^3S_1$ is metastable with a typical lifetime in an active discharge on the order of a fraction of a millisecond, limited by collisions with other discharge products and/or container walls. As a consequence, the $2\,^3S_1$-state population in the discharge ($10^{10}$–$10^{11}$ cm$^{-3}$) is much greater than that of other excited states. In the discharge, several two-step ionization processes involving atoms in this metastable state are possible, as well as is direct electron-impact ionization of ground-state atoms. These cumulative processes involve, first, the creation of a long-lived metastable state by electron-impact excitation, and then subsequent ionization in a second reaction. At the low gas pressures (< 1 torr) with which we are concerned, associative ionization processes[3] and three-body reactions can be neglected.

The relative importance of cumulative ionization processes can be determined by using spin polarization to "label" the electrons associated with the metastable atoms. Previous experiments have shown that optical pumping in a helium discharge can produce a high degree of electron spin polarization in the triplet metastable atoms.[4,5] Ionization reactions involving this optically pumped state will yield polarized electrons if the reactions conserve spin angular momentum. Thus by extracting the electrons produced in such a discharge and measuring their spin polarization, the importance of cumulative ionization involving the $2\,^3S_1$ state can be determined.

To perform these experiments we have used a conventional helium optical-pumping apparatus[5]; this consists of a cell containing helium gas subjected to electrical discharge, irradiated by polarized 1.08-$\mu$ $2\,^3S$-$2\,^3P$ resonance light. However, we modify the cell by attaching a base plate with a hole through which the electrons can be extracted for subsequent analysis. The electron polarization is measured by Mott scattering at 120-keV energy from a thin gold foil.

The measurements show that the electrons extracted from an active helium discharge may have a large polarization, indicating that cumulative ionization processes play a substantial role. Electrons extracted from the afterglow of a pulsed discharge, where the electron production mechanisms are known to be cumulative, show even higher polarizations. These measurements also provide strong evidence that spin conservation holds for the ionization reactions.

There has been great interest during recent years in the use of polarized electron beams for atomic and high-energy nuclear scattering experiments.[6] The procedure described here can be used to produce an electron beam that has an intensity substantially greater than any other system yet developed. In addition, the source is easy to operate and allows the electron spin direction to be easily inverted without altering the beam trajectory. This

method is technically simple, inexpensive, and appears to be suitable for use in low-energy electron-atom collision experiments and with high-energy electron accelerators.

In this paper we first discuss the significant electron production mechanisms in the discharge and compare their relative efficiencies. We then review the optical-pumping process and outline a method by which the magnetic sublevel population distribution of the optically pumped $2\,^3S_1$ state can be computed; from a knowledge of this population distribution, the polarization of the electrons produced by cumulative ionization processes can be determined. Finally we present experimental results, which show the electron polarization in the active discharge as a function of discharge intensity, gas pressure, base-plate material, and base-plate geometry. Other measurements show the polarization of electrons extracted from the afterglow of a pulsed discharge as a function of gas pressure and of time in the afterglow.

## II. DISCHARGE PROCESSES

In this section the relative importance of competing ionization mechanisms in an active discharge will be considered. Under steady-state conditions these mechanisms can be analyzed by balancing the electron production rate against the rate of electron loss. The importance of cumulative ionization processes in high-frequency helium discharges can be emphasized by reviewing the mechanics of a radio-frequency discharge. A free electron in the gas is set into oscillation by the external electric field; in the absence of collisions its velocity is out of phase with the applied field and no net power is absorbed during the cycle. Collisions with ground-state atoms alter the momentum of the oscillating electron so that there arises a velocity component perpendicular to the applied field. Since the average energy accumulated in each collision is very small,[7] many such randomizing collisions are required before the electron reaches the first excitation threshold of 19.8 eV. As the energy of the electron increases above this value, more and more excited states become accessible, so that the effective electron deexcitation cross section increases rapidly with increasing energy. In the discharge, therefore, the number of electrons with energy above 19.8 eV should be a rapidly decreasing function of energy. This qualitative picture is consistent with quantitative calculations of the electron energy distribution in a high-frequency discharge.[8]

### A. Electron Production and Loss in an Active Discharge

#### 1. *Direct Ionization*

Electron-impact ionization can occur directly in collisions between electrons and ground-state helium atoms, provided the energy of the incoming electron is greater than 24.5 eV, the ionization threshold. The production rate for this process can be written

$$\left(\frac{dn_e}{dt}\right)_1 = \bar{\sigma}_1 \bar{v} N n_e(>24.5)\,, \tag{1}$$

where[9] $\bar{\sigma}_1 \simeq 3\times10^{-18}$ cm$^2$ is the cross section averaged over the distribution of electron velocities, $\bar{v}$ is the average relative velocity of the two particles, $N$ is the ground-state helium density, and $n_e(>24.5)$ is the density of electrons with energy greater than 24.5 eV.

#### 2. *Cumulative Ionization*

Cumulative processes involving the $2\,^3S_1$ and $2\,^1S_0$ metastable states will predominate because of their high populations compared to other excited states. The relative populations of these two states in a typical discharge is measured by optical absorption of the $2\,^3S \rightarrow 2\,^3P$ and $2\,^1S \rightarrow 2\,^1P$ lines to be approximately in the ratio of their statistical weights (3:1). The electron production rate from electron-impact ionization of these metastable atoms is calculated just as for the direct case. The reaction is

$$\mathrm{He}^M + e^- \rightarrow \mathrm{He}^+ + 2e^-\,,$$

where $M$ denotes either the triplet ($T$) or singlet ($S$) metastable state, with densities $N_T$ and $N_S$, respectively.

The electron production rates are

$$\left(\frac{dn_e}{dt}\right)_2 = \bar{\sigma}_2 \bar{v}_e N_T n_e(>4.7) \tag{2}$$

and

$$\left(\frac{dn_e}{dt}\right)_3 = \bar{\sigma}_3 \bar{v}_e N_S n_e(>3.8) \tag{3}$$

for $2\,^3S$ and $2\,^1S_0$ metastables, respectively. The average cross section[10] $\bar{\sigma}_2 = \bar{\sigma}_3 \cong 6\times10^{-18}$ cm$^2$ will be used for both reactions.

The only other important production mechanism in a low-density helium discharge is the collision between two metastable atoms

$$\mathrm{He}^M + \mathrm{He}^M \rightarrow \mathrm{He}(1\,^1S_0) + \mathrm{He}^+ + e^-\,.$$

For this mechanism

$$\left(\frac{dn_e}{dt}\right)_4 = \bar{\sigma}_4 \bar{v} (N_M)^2\,, \tag{4}$$

where $N_M = N_T + N_S$ is the total metastable density. The cross section for this reaction[11] is about $10^{-14}$ cm$^2$, yielding, for an average relative velocity at thermal energies of about $2\times10^5$ cm sec$^{-1}$,

$$\frac{dn_e}{dt} \simeq 2\times 10^{-9}(N_M)^2 . \quad (5)$$

The density of metastable atoms in the discharge can be computed from a measurement of the fractional absorption of the 1.08-$\mu$ resonance radiation used to optically pump the atoms in the $2\,^3S_1$ state.[12] This calculation indicates[13] that at the discharge intensity at which we measured maximum electron polarization (see Sec. V) the density of the atoms in the $2\,^3S_1$ state is about $6\times 10^{10}$ cm$^{-3}$, and we use this value below for computing representative electron production rates. However, the error in this number could be rather large because of uncertainties in the spectral profile of the lamp (see the Appendix) and in the distribution of metastables throughout the source gas.

In estimating electron-impact production rates we substitute a velocity which corresponds to an energy just above the threshold for each process, yielding production rates for direct and cumulative processes:

$$\left(\frac{dn_e}{dt}\right)_1 \simeq 9\times 10^{-10} N_{\mathrm{He}} n_e (>24.5) \quad \text{(direct)}, \quad (6)$$

$$\left(\frac{dn_e}{dt}\right)_2 \simeq 3.2\times 10^{3} n_e (>4.7) \quad (e\text{-triplet } MS), \quad (7)$$

$$\left(\frac{dn_e}{dt}\right)_3 \simeq 1.0\times 10^{3} n_e (>3.8) \quad (e\text{-singlet } MS), \quad (8)$$

$$\left(\frac{dn_e}{dt}\right)_4 \simeq 1.3\times 10^{13} \quad \text{(metastable-metastable)}. \quad (9)$$

### 3. *Electron Loss*

We have investigated discharges in the pressure range from 0.035 to 1.0 torr. At these low pressures, bulk recombination of electrons and ions can be neglected, and electron loss occurs predominately through ambipolar diffusion to the cell walls, where recombination occurs. For the 100-cm$^3$ spherical cells used in these experiments the characteristic diffusion length for the lowest mode is $\Lambda_0 = 0.78$ cm. By neglecting higher diffusion modes, a lower limit on the electron loss rate is established as

$$\frac{dn_e}{dt} \geq \frac{n_e}{\tau_0} ,$$

where $\tau_0 = \Lambda_0^2/D_a$ is the characteristic decay time of the lowest diffusion mode.

The ambipolar diffusion coefficient $D_a$ is related to the free-ion diffusion coefficient $D_+$ by the relation $D_a = D_+(1 + T_e/T_+)$, where $T_e$ and $T_+$ are the "temperatures" which characterize the average energy of the electrons and ions in the cell.[14] For the calculations reported here we have used the results of Oskam's[15] measurements of the effective $He^+$ mobility[16] $\mu_+$ and the Einstein relation $D_a = kT^*/\mu_+ e$ to determine the value of $D_a$.

In this laboratory the electron temperature $T_e$ in the discharge has not been measured, but is known always to be a few eV on the basis of other experiments.[17] Using the above procedures we calculate that at 0.1 torr (the pressure at which maximum electron polarization was observed) the value of $D_+$ is about $2.3\times 10^3$ cm$^2$ sec$^{-1}$. Estimating the average electron energy as about 2.5 eV we compute that $D_a = 2.3\times 10^5$ cm$^2$ sec$^{-1}$; therefore in an active discharge $\tau_0 \leq 3\times 10^{-6}$ sec, and the electron loss rate is

$$\frac{dn_e}{dt} \geq 3\times 10^5 n_e \ \mathrm{sec}^{-1} . \quad (10)$$

It is immediately apparent that steady-state electron production by electron-impact ionization of $2\,^1S_0$ and $2\,^3S$ metastable atoms [Eqs. (7) and (8)] cannot possibly support the much larger loss rate computed above. Furthermore, if direct ionization [Eq. (6)] is to be significant at the 0.1-torr ($\sim 3.5\times 10^{15}$ atoms/cm$^3$) gas pressure under consideration, then approximately 10% of the electrons in the discharge must have energy greater than the 24.5-eV threshold. This would appear to be an improbably large percentage of high-energy electrons in a weak discharge in view of the earlier discussion of discharge mechanics.[18] Thus, metastable-metastable collisions [Eq. (9)] remain as the most likely source of electrons in the discharge. Equating the loss rate to the electron production rate by metastable-metastable reactions yields a steady-state electron density of about $4\times 10^7$ cm$^{-3}$. This is in good agreement, in view of uncertainties in calculations of metastable density and electron loss rate, with a directly measured value of $7\times 10^7$ electrons/cm$^3$ for a discharge operated in this laboratory under experimental conditions very similar to those of the present experiment.[19]

## B. Afterglow Electron Production and Loss Mechanisms

Ionization reactions involving electron impact do not occur in the afterglow since the electrons rapidly come to thermal equilibrium with the gas atoms after the source of excitation is removed. However, the metastable-metastable reaction continues to produce electrons for as long as the metastables exist in significant concentrations. The metastable lifetime, which is limited only by the diffusion time to the walls, is on the order of $10^{-4}$ to $10^{-3}$ sec for the experimental conditions reported here.[17,20]

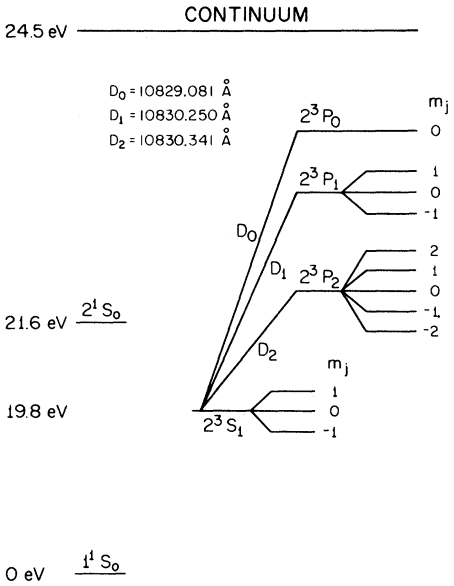


FIG. 1. Helium energy-level diagram (not to scale). The three components of the pumping light are labeled $D_0$, $D_1$, and $D_2$. The optical pumping cycle tends to increase the population of the $m=+1$ sublevel of the $2\,^3S_1$ state (for right circularly polarized light) or the $m=-1$ sublevel (for left circularly polarized light).

Furthermore, since the electrons come to thermal equilibrium with the gas atoms the ambipolar diffusion coefficient is greatly reduced. Under these conditions the loss rate may be on the order of 100 times smaller than in the active discharge.[17] Late in the afterglow any free electrons must certainly have been produced by metastable-metastable reactions.

Our conclusion, then, is that under the conditions of the present experiment, metastable-metastable reactions are the primary source of electrons in the active discharge, just as in the afterglow. As will be shown in Sec. III, the electrons produced in this way will be spin oriented if the metastable atoms are optically pumped and spin conservation holds for the reactions.

### III. OPTICAL PUMPING IN HELIUM

The population distribution in the optically pumped $2\,^3S_1$ state can, in principle, be determined from measurements of absorption of the 1.08-$\mu$ pumping radiation by the sample. In these experiments, helium gas is contained in a 100-cm$^3$ spherical Pyrex bulb at pressures ranging from 0.035 to 1.0 torr. A weak rf discharge produces a steady-state $2\,^3S_1$ population in the range $10^{10}$–$10^{11}$ cm$^{-3}$. Because of their short radiative lifetimes, other excited states are populated to a much lesser extent, with the exception, of course, of the $2\,^1S_0$ state. Circularly polarized 1.08-$\mu$ resonance radiation from a helium discharge lamp is then used to excite the $2\,^3S_1$-$2\,^3P_{0,1,2}$ transitions (see Fig. 1). This imposes the selection rule $\Delta m=+1$ for right circular polarization (or $-1$ for left circular polarization). Spontaneous decay to the $2\,^3S_1$ level obeys the selection rule $\Delta m=\pm 1$ or 0. This cycle tends to increase the magnetic quantum number $m$ of a typical metastable atom (for right circularly polarized light). In other words, angular momentum from the pumping light is transferred to the atomic electrons.

This process of preferential population of the magnetic sublevels must compete with any thermalizing process which tends to restore the normal Boltzmann distribution. Pumped metastables are lost by diffusion to the walls; they are replaced by unpolarized metastables produced by electron-impact processes. At pressures above 0.5 torr collisional mixing in the $2\,^3P$ states prior to decay[21] reduces the effectiveness of the optical-pumping process.

Following Schearer,[5] the rate equations that describe the sublevel population changes in the $2\,^3S_1$ state during the pumping process for an optically thin sample are

$$\frac{dN_i}{dt}=-FN_i\sum_{k=1}^{9}B_{ik}+F\sum_{j,k=1}^{k=9,j=3}B_{jk}A_{ki}N_j+\frac{\frac{1}{3}N-N_i}{\tau}\,, \tag{11}$$

where $F$, which is proportional to the pumping light intensity, characterizes the rate of absorption of the pumping radiation; $N_i$ is the population density of the $i$th metastable sublevel, and $N=\sum_{i=1}^{3}N_i$; $B_{ik}$ is the relative absorption probability between the $i$th $2\,^3S_1$ sublevel and the $k$th $2\,^3P$ sublevel; $A_{ki}$ is the relative spontaneous transition probability between the $k$th $2\,^3P$ and $i$th $2\,^3S$ sublevels; and $\tau$ is the characteristic lifetime due to thermalization processes of an atom in a particular $2\,^3S$ sublevel.

The spectrum of the $2\,^3S_1$-$2\,^3P$ resonance radiation actually consists of three lines labeled $D_0$, $D_1$, and $D_2$, corresponding to transitions from the three separate $P$ sublevels. The $D_1$ and $D_2$ transitions, however, are not resolvable. The precise intensity of these lines in the pumping radiation, relative to their corresponding absorption lines, is not well known because of slight pressure- and intensity-dependence of the spectral-line positions and shapes[22]; therefore parameters $K$ and $L$ are introduced, so that the intensities of pumping radiation exciting $D_0$, $D_1$, and $D_2$ transitions are in the ratio $K:L:1$ (see the Appendix). The population for each level $N_i$ can then be evaluated by substituting the appropriate values of $B_{ik}$ and $A_{ki}$ from Tables I and II into the rate equations and then imposing the steady-state condition $dN_i/dt=0$. This

TABLE I. Relative absorption probabilities for pumping-radiation intensity distribution characterized by $D_0$: $D_1$: $D_2 = K$: $L$:1.

| | $B_{ik}$ | $2\,^3P_2$ | | | | | $2\,^3P_1$ | | | $2\,^3P_0$ |
|---|---|---|---|---|---|---|---|---|---|---|
| | $i$ \ $k$ | 2 | 1 | 0 | −1 | −2 | +1 | 0 | −1 | 0 |
| $2\,^3S_1$ | +1 | 6 | 0 | 0 | 0 | 0 | 0 | 0 | 0 | 0 |
| | 0 | 0 | 3 | 0 | 0 | 0 | $3L$ | 0 | 0 | 0 |
| | −1 | 0 | 0 | 1 | 0 | 0 | 0 | $3L$ | 0 | $2K$ |

yields

$$N_+ = (2N/\Delta)\,[1 + \tfrac{1}{2}\tau F(8 + 12L + 4K) + \tfrac{3}{4}(\tau F)^2(1+L)(5+9L+8K)]\,,$$

$$N_0 = (2N/\Delta)[1 + \tfrac{1}{2}\tau F(3 + 3L + 4K)]\,, \qquad (12)$$

$$N_- = (2N/\Delta)[1 + \tfrac{1}{2}\tau F(3 + 3L)]\,,$$

where

$$\Delta = \tfrac{3}{2}(\tau F)^2(1+L)(5+9L+8K) + \tau F(14 + 18L + 8K) + 6\,. \qquad (13)$$

The pumping process can be characterized experimentally by the intensity of the 1.08-$\mu$ light which passes through the discharge cell. The optical signal $\Delta I$ is determined by subtracting the light intensity transmitted through pumped metastables from the transmitted intensity when the metastables are depumped. The metastables are depumped by saturation of the $\Delta m = \pm 1$ magnetic dipole transitions with an externally imposed resonant rf magnetic field.

The optical signal $\Delta I/I_0$, normalized to the intensity of the incident light can be written as

$$\Delta I/I_0 = \textstyle\sum_l \Delta I^{(l)} / \sum_l I_0^{(l)} = \sum_l (I^{(l)} - I_0^{(l)})/I_0\,, \qquad (14)$$

where $I^{(l)}$ and $I_0^{(l)}$ represent the total light absorbed by the $D_l$ component in the unpumped and pumped conditions, respectively, and $\sum_l I_0^{(l)} = I_0$. Since the fractional absorption of each component is proportional to the absorption probability for the level times the level population, the resulting terms for $I_0^{(l)}$ and $I^{(l)}$ are

$$I_0^{(0)} \sim (2K)\tfrac{1}{3}N\,, \quad I^{(0)} \sim (2K)N_-\,;$$

$$I_0^{(1)} \sim (6L)\tfrac{1}{3}N\,, \quad I^{(1)} \sim 3L(N_0 + N_-)\,; \qquad (15)$$

$$I_0^{(2)} \sim (10)\tfrac{1}{3}N\,, \quad I^{(2)} \sim 6N_+ + 3N_0 + N_-\,.$$

Using the previously calculated values for $N_i$ the total observed signal is

$$\frac{\Delta I}{I_0} = \frac{K(5+9L+8K)}{10+6L+2K} \times \frac{2\tau F + 3(\tau F)^2(1+L)}{6 + \tau F(14+18L+8K) + \frac{3}{2}(\tau F)^2(1+L)(5+9L+8K)}\,. \qquad (16)$$

The experimentally accessible quantity is $\Delta I/I_0$. Thus, $(\tau F)$ and then the level population ratios $N_+ : N_0 : N_-$ can be computed from Eqs. (16) and (12), for selected values of the parameters $K$ and $L$ (see the Appendix for a discussion of the range of possible values of these parameters).

Finally, these values of the sublevel population distribution can be used to compute the expected electron polarization from spin-conserving ionization reactions involving the $2\,^3S$ state. In particular, we are interested in electrons produced by metastable-metastable collisions. Our calculation includes the contribution from the unpumped singlet ($2\,^1S_0$) metastable atoms (labeled $N_s$ below). Assuming equal cross sections for all processes except those not allowed by spin angular momentum conservation,[23] the total production rates for electrons with spin projections "up" ($n_u$) and "down" ($n_d$) are, respectively,

$$\frac{dn_u}{dt} \sim \tfrac{1}{2}N_S^2 + N_0 N_S + 2N_S N_+ + 2N_+ N_0 + N_+ N_- + \tfrac{1}{2}N_0^2\,,$$

$$\frac{dn_d}{dt} \sim \tfrac{1}{2}N_S^2 + N_0 N_S + 2N_S N_- + 2N_0 N_- + N_+ N_- + \tfrac{1}{2}N_0^2\,. \qquad (17)$$

The free-electron polarization is defined as

$$P_e = (n_u - n_d)/(n_u + n_d)\,. \qquad (18)$$

Substituting the values from the above equations we get

$$P_e = \frac{2(N_0 + N_S)(N_+ - N_-)}{(N_S + N_+ + N_0 + N_-)^2 - N_+^2 - N_-^2}\,. \qquad (19)$$

(A similar calculation for electron-metastable collisions shows that there should be little difference in the polarization of electrons produced by the two reactions.)

From the measured values of $\Delta I/I_0$, we have computed the metastable sublevel populations for the range of reasonable values of $K$ and $L$. The results of this computation are shown in Fig. 2 along with the measured $\Delta I/I_0$ values, for $K : L : 1$

TABLE II. Relative $2\,^3P_{0,1,2} \rightarrow 2\,^3S_1$ spontaneous transition probabilities.

| | $A_{jk}$ | $2\,^3P_2$ | | | | | $2\,^3P_1$ | | | $2\,^3P_0$ |
|---|---|---|---|---|---|---|---|---|---|---|
| | $j$ \ $k$ | 2 | 1 | 0 | −1 | −2 | +1 | 0 | −1 | 0 |
| $2\,^3S_1$ | +1 | 6 | 3 | 1 | 0 | 0 | 3 | 3 | 0 | 2 |
| | 0 | 0 | 3 | 4 | 3 | 0 | 3 | 0 | 3 | 2 |
| | −1 | 0 | 0 | 1 | 3 | 6 | 0 | 3 | 3 | 2 |

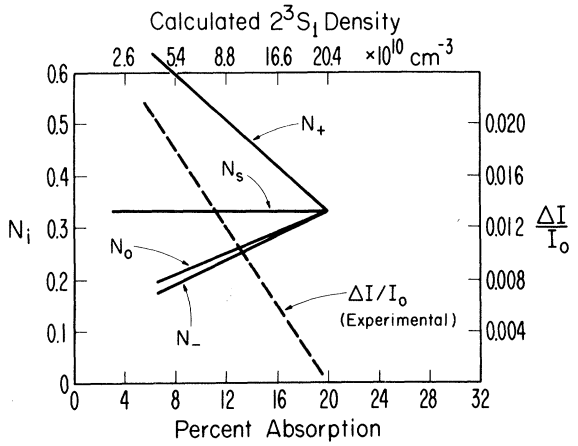


FIG. 2. Calculated values of the relative populations $N_+$, $N_0$, and $N_-$ of the $2\,^3S_1$ magnetic sublevels $m=+1$, 0, $-1$, respectively. The abscissa is the relative absorption of the 1.08-$\mu$ pumping light which characterizes the discharge intensity and from which the $2\,^3S_1$ density can be estimated. The dashed curve shows the measured optical-pumping signal $\Delta I/I_0$. The population distribution is computed using Eqs. (12) and (17) and using $K:L:1 = 0.4:1.3:1$, the best estimate.

$= 0.4:1.3:1$. The anticipated electron polarizations determined for the entire range of $K$ and $L$ values are shown in Fig. 3. The uncertainty in the $K$ and $L$ values is about $\pm 30\%$ (see the Appendix). In all cases we expect a substantial electron spin polarization which increases as the size of the pumping signal $\Delta I/I_0$ increases. Because the $K$ and $L$ components of the pumping light are absorbed at different rates,[5] the estimated polarizations (as well as computed $2\,^3S_1$ densities) are most accurate at the lower discharge levels; i.e., the equations apply well only when the sample is optically thin. The measurement errors of $\Delta I$ and $I$ are approximately $\pm$ 15% and 5%, respectively.

The electron polarization actually measured in the analyzed beam can be expected to be diminished by admixture of secondary electrons resulting from collisions of metastables and ions with the walls of the exit canal[24]; this will be considered in greater detail in Sec. V.

It should be noted that electron exchange reactions of the form

$$He^T(\uparrow\uparrow) + e^-(\downarrow) \rightarrow He^T(\uparrow\downarrow) + e^-(\uparrow)\,,$$

where $(\uparrow)$ labels the electron spin orientation, can in principle also contribute to the observed polarization. However, despite its large cross section ($\sigma_{ex} \simeq 1.6\times 10^{-14}$ cm$^2$ at thermal energies),[25] this process is quite ineffective in these experiments because the mean exchange time $\tau_{ex} = (\sigma_{ex}\bar{v}N_T)^{-1} \simeq 6\times 10^{-5}$ sec is much longer than the average electron lifetime of $\lesssim 3\times 10^{-6}$ sec computed earlier. Furthermore, it is unlikely that the large thermal-energy value of $\sigma_{ex}$ persists at the higher ($\sim$ 2.5 eV) energies of these experiments, so that $\tau_{ex}$ is in all likelihood underestimated. Finally, the electrons actually spin analyzed are extracted from a small volume very near the exit canal, where their average dwell time is substantially less (probably by a factor of about 100) than the average lifetime of electrons in the cell.[26]

## IV. EXPERIMENTAL APPARATUS

The optical-pumping apparatus and the electron extraction electrode are shown in Fig. 4, and a schematic diagram of the entire experiment is shown in Fig. 5. The discharge cell is a Pyrex sphere about 5 cm in diam; it is attached to a metal base plate through which a hole is drilled so that the electrons in the discharge can be extracted and analyzed. An electrical discharge is maintained in the gas by a capacitively coupled 50-MHz oscillator. Helmholtz coils produce a small magnetic field (nominally 5 G) in a direction parallel to the incident pumping light so that a unique spin quantization axis is defined.

The 1.08-$\mu$ resonance radiation necessary for optical pumping is produced by a high-intensity helium discharge lamp. The resonance light is circularly polarized by a linear polarizer and quarter-wave plate. The sense of circular polarization can be reversed during the experiment by a 90° rotation of the linear polarizer. Light from the lamp which passes through the discharge is focused upon a PbS photodectector, so that the metastable helium polarization can be determined by measurement of the transmitted light, as de-

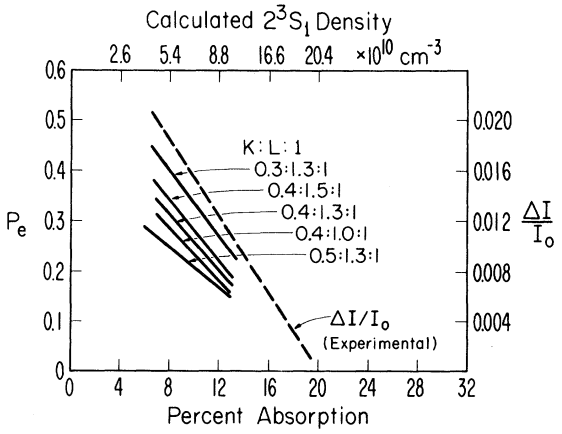


FIG. 3. Computed values of the electron polarization for metastable-metastable ionization reactions [Eq. (20)]. To account for uncertainties in the intensities of the pumping-light components, the calculation is done for several values of the ratios $K:L:1$.

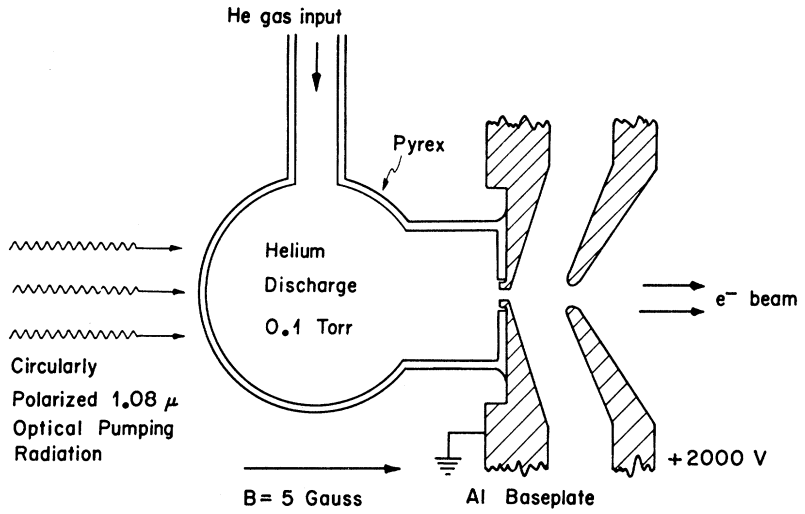


FIG. 4. Schematic diagram of the optical-pumping cell attached to the metal base plate. Also shown is the electrode used to extract the electrons from the discharge.

scribed in Sec. III. Contaminants can shorten the effective metastable lifetime and consequently diminish the ultimate $2\,^3S_1$ polarization; therefore, high-purity (< 3 ppm) helium is admitted to the sample cell through a cryogenic trap. The input line and cell are periodically baked to reduce the contribution of outgassing from the walls.

The free electrons in the discharge are extracted with an electrode that is normally biased to + 1900 V relative to the base plate. The extracted current depends, of course, upon the gas pressure, the intensity of the discharge, and the potential of the extractor. For these experiments no significant effort has been made to optimize the extracted current. In order to reduce the number of secondary electrons produced at the exit canal, its diameter was made as large as possible. The maximum size of this hole is restricted only by the pumping-speed limitations of the pumps which evacuate the electron optical system.

Before acceleration to 120 keV for Mott analysis of the electron polarization, the beam passes through an electron filter lens.[27] This is used not only to focus the beam but also to determine the energy distribution of the extracted electrons. The calculated energy resolution of the lens is about 0.2%, or about 4 eV for 1900 electrons.

For studies of the electron polarization in the discharge afterglow, a pulse generator is used to trigger the discharge oscillator. The electrons extracted from the afterglow can be isolated by synchronously pulsing the retarding plane (center

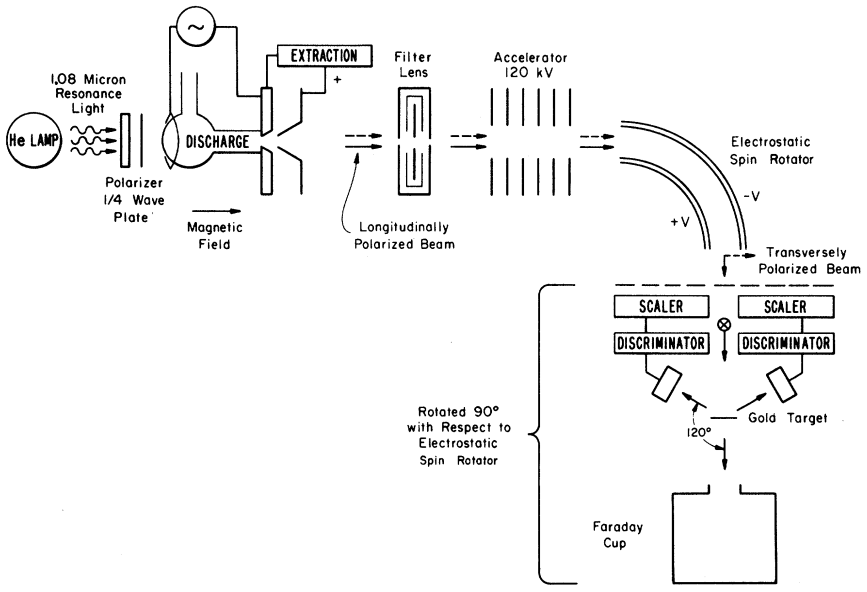


FIG. 5. Schematic diagram of the experiment (not to scale).

electrode) of the filter lens. The delay and width of the filter-lens transmission can be adjusted so that the electrons can be sampled at any time in the afterglow.

The entire optically pumped electron source, extraction optics, and filter lens, together with associated electronics and pumps for evacuating the extraction region and accelerator column, are mounted on a large table which is biased to a potential of $-120$ kV relative to the laboratory ground.

After leaving the filter lens the electrons pass through an accelerating column[28] to ground potential where they are analyzed. Because the electrons are extracted in a direction parallel to the applied magnetic field and pumping light, they are longitudinally polarized; after acceleration they are rotated to the transverse direction required for Mott analysis by a cylindrical-plate spin rotator.[29] The measured energy resolution of the spin rotator is about 4% and the transmission is approximately 30%.

Mott scattering has been used previously by others both to measure the spin polarization of electrons emitted in $\beta$-decay processes and to test several methods of producing polarized electron beams. The principle, first proposed by Mott in 1929,[30] is that a small azimuthal scattering asymmetry due to spin-orbit effects will appear in the usual Rutherford scattering pattern when a beam of transversely polarized electrons is scattered by the Coulomb field of a heavy nucleus. Recent experiments by van Klinken[31] and Mikaelyan[32] have shown close correspondence with the theoretical values[33,34] for the scattering asymmetry.

In this experiment the electrons to be analyzed are scattered from a gold target into two silicon surface-barrier detectors placed symmetrically at a scattering angle of $\theta = 120°$ and azimuthal angles relative to the vertical of $0°$ and $180°$, respectively; the electron energy is 120 keV. The scattering asymmetry is characterized by a function $S(\theta)$, such that the ratio of counting rates in the two detectors is

$$R_1/R_2 = [1 + S(\theta)P_e]/[1 - S(\theta)P_e] , \qquad (20)$$

where the electron polarization is $P_e = (n_u - n_d)/(n_u + n_d)$, and $n_u$ and $n_d$ are the relative numbers of transversely polarized electrons with spin axes at azimuthal angles of $90°$ and $270°$, respectively. Thus $P_e$ can be determined from a measurement of the scattering asymmetry.

The most serious errors in any experiment involving Mott scattering are usually due to instrumental asymmetries. In this experiment, however, the sense of circular polarization of the optical-pumping radiation can be reversed simply by rotating the linear polarizer in the light path by $90°$. This reverses the electron polarization direction in the extracted beam by $180°$, without affecting the instrumental geometry in any portion of the beam path. Instrumental asymmetries can therefore be eliminated from the analysis by averaging the counting rate ratios $R_1$ and $R_2$ for the two senses of optical polarization. Each value of the polarization reported in Sec. V is the average of eight sets of such measurements; the reported error is the standard deviation of the eight individual polarization measurements. In every case this deviation was significantly greater than the internal statistical error[35]

$$\Delta P_e = \left[ \frac{1}{n_u + n_d} \left( \frac{1}{S(\theta)^2} - P_e^2 \right) \right]^{1/2} . \qquad (21)$$

Presumably the fluctuations in the beam polarization are due to small instabilities in the discharge, particularly in the region of the exit canal.

The cylindrical Mott scattering chamber has an inside diameter of 20 cm and an inside height of 20 cm. A Faraday cup 30 cm from the gold target is used to monitor the beam current passing through the target foil. To minimize the effect of elastically back-scattered electrons, all surfaces exposed to the primary beam of scattered electrons are coated with graphite (Aquadag).

The self-supporting gold-leaf targets used in this experiment have a thickness of $193 \pm 5$ $\mu g/cm^2$. These relatively thick targets yield high counting rates; however, they also introduce a high rate of multiple scattering within the target. To account for this contribution we have used the results of an extrapolation to zero target thickness obtained by Kessler[36] for this angle and energy ($120°$ and 120 keV). This extrapolation reduces the effective value of the asymmetry function $S(\theta)$ used in the analysis from 0.378 to 0.26.

## V. EXPERIMENTAL RESULTS

The electron polarization was measured over a wide range of discharge intensities as well as at several different gas pressures. The effect of secondary electrons produced near the exit canal was studied by varying the base-plate material and geometry. In addition, the dependences of the polarization upon time and gas pressure in the afterglow of a pulsed discharge were measured.

### A. Steady-State Discharge

Figure 6 shows the polarization of the electrons extracted from an active discharge displayed as a function of discharge intensity at a helium pressure of 0.08 torr,[37] where optimum polarization was obtained. The figure also shows extracted electron currents. The large electron polarization measured indicates that the assumption of spin conservation in electron production reactions involving optically pumped metastables is at least partially correct.

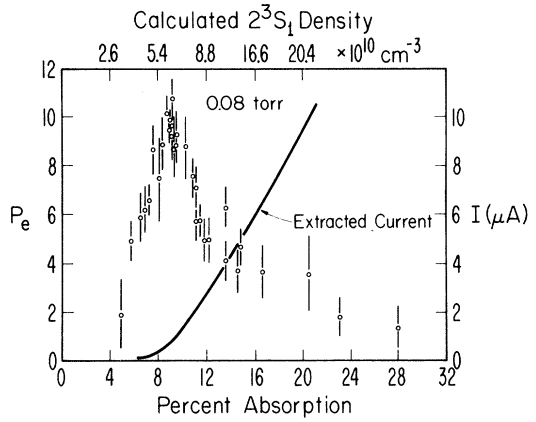


FIG. 6. Observed polarization and beam intensity of electrons extracted from an active discharge vs discharge intensity. The gas pressure is 0.08 torr. As in Figs. 1, 2, and 3 the relative absorption of the 1.08-$\mu$ pumping light characterizes the discharge intensity.

It can definitely be concluded that cumulative ionization processes involving metastable $2\,^3S_1$ atoms play a major role in weak helium discharges at this pressure. A maximum polarization of 10.0 $\pm$0.5% was observed with an extracted beam current of 0.2 $\mu A$. It should be noted that much larger beam currents can be extracted, with only modest loss of polarization, at somewhat higher discharge levels.

Because of the large number of competing processes which contribute to the discharge and extracted current, it is difficult to make a detailed quantitative interpretation of the dependence of polarization on discharge intensity (i.e., upon percent absorption of pumping radiation). However, general features of the curves can be understood qualitatively.

The declining polarization at low-discharge levels presumably results because electron production by reactions that produce polarized electrons decreases more rapidly with declining discharge levels than does the production of unpolarized electrons. For example, metastables (and ions) striking the metal extraction canal can be expected to give rise to secondary electrons which will be extracted (with unknown efficiency) along with electrons produced by reactions in the discharge. The secondary electrons are presumably unpolarized.[38] Secondary electron production by metastable-exit-canal collisions depends linearly upon metastable density whereas the production rate in the discharge by metastable-metastable reactions is proportional to the metastable density squared. Note that at the lower discharge levels the electron current appears to have the parabolic dependence on metastable density that would be expected from metastable-metastable reactions.

The flux of metastables diffusing to the ~0.1-cm$^2$ extraction area is estimated to be about $4\times10^{13}$ sec$^{-1}$ for experimental conditions where the observed electron polarization is optimum. With a conversion efficiency to electrons of about 0.28,[24] this gives rise to a production rate of a little over $10^{13}$ secondary electrons per second. We conclude that only a small fraction of these are extracted, however, since the total extracted current is only about 0.2 $\mu A$, or about $10^{12}$ electrons/sec. Electrons produced by ion collisions with the canal probably can be ignored, since the charge neutrality in the discharge allows the production rate by this process to be no greater than the total extracted current. The extraction efficiency for ion-produced secondaries should be comparable to that for metastable-produced secondaries.

The decrease in the electron polarization at high discharge levels is in general agreement with the observed behavior of the optical pumping signal $\Delta I/I_0$, which indicates a steady diminution of $2\,^3S_1$ polarization with increasing discharge intensity. Several processes may contribute to the $2\,^3S_1$ polarization degradation, the most serious of which is probably the depumping effect associated with significant trapping at high metastable densities of the $2\,^3P$-$2\,^3S$ resonance radiation emitted in the optical-pumping cycle.[39] It is probable that the mean free path of the fluorescent photons is substantially less than for the photons in the pumping light because of the narrower spectral width and unshifted position of the fluorescent lines.

A second detrimental process is the electron-impact excitation of the $2\,^3S$ metastables, which becomes increasingly important as the discharge level, and hence the electron density, is increased. These collisions tend to randomize the spin orientation of the excited electrons. For example the reaction $\mathrm{He}(2\,^3S_1)+e^-\rightarrow \mathrm{He}(2\,^3P)+e^-$ has a calculated cross section of $\sim 2\times10^{-14}$ cm$^2$ over a wide range of electron energies above the ~1-eV threshold.[40]

Measurements of electron polarization and extracted beam current were also made as a function of discharge intensity for source-gas pressures both higher and lower than the 0.08-torr pressure at which maximum polarization was obtained. The data shown in Fig. 7 for pressures of 0.035 and 0.11 torr are representative. The 0.08-torr data are repeated for comparison. While the general features of the data at all pressures are similar, it is seen that the extracted current for a particular metastable density rises rapidly at low pressures, while the polarization is only slightly degraded. A 4-$\mu A$ beam with 8% polarization was extracted at 0.035 torr.[41] The reduction in polarization can be attributed to the shorter metastable lifetimes at lower pressures resulting from their rapid diffusion to the cell walls where deexcitation

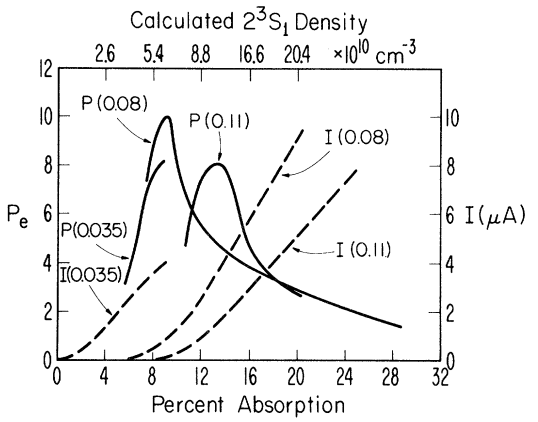


FIG. 7. Observed electron polarizations and beam intensities vs discharge intensity for active discharges at pressures of 0.035 and 0.11 torr. Smoothed data for 0.08 torr from Fig. 6 are included for comparison. For clarity the error bars have been removed; errors are comparable to those indicated in Fig. 6.

occurs. This reduces the relaxation time $\tau$ of the $2\,^3S_1$ polarization, and thus tends to short circuit the optical-pumping process [see Eq. (12)].

The falloff in polarization at high pressures is not completely understood, but is at least partially explained by the increasing collisional mixing rate in the optically excited $2\,^3P$ states, which depends linearly on the pressure.[21,42] The extraction efficiency is also degraded at the higher pressures, so that the relative admixture of secondary electrons in the electron beam may be greater.

The above measurements were made by extracting the electrons through a 2-mm-diam by 2-mm-long exit canal (see Fig. 4). The exit-canal geometry and material were varied in an attempt to better elucidate the contribution of secondary electrons. Substituting an exit canal 1 mm in diam and 1 mm in length resulted in substantially lower polarizations and beam intensities. This is consistent with the expectation that the relative contribution of secondary electrons produced at the exit canal should increase for smaller exit-canal diameters. No differences in polarization or extracted current were observed for exit canals constructed of copper, aluminum, and graphite.

By using the filter lens as an analyzer, electron polarization was measured as a function of energy of the extracted electrons. No dependence upon energy was observed. The spread in electron energies was found in the course of this investigation to be of the order of 10 to 15 eV. It was hoped initially that the contribution of secondary electrons could be discriminated aginst with an energy filter, but the results suggest that the energy distributions of both primaries and secondaries are probably determined more by the extraction technique than by their production mechanisms. This subject probably should be explored further with different extraction conditions.

### B. Discharge Afterglow

When the discharge is terminated by removal of the excitation source, residual ions and electrons diffuse to the container walls where they recombine. However, production of new electrons through metastable-metastable reactions persists for a period comparable to the metastable diffusion time to the walls. Thus, in contrast to the active discharge, metastable-metastable reactions are isolated as the only source of electrons during the afterglow period.[17] Furthermore, the absence of hot electrons and extraneous discharge products that might have a deleterious effect on the optical-pumping process can only lead to an increase in the polarization of the $2\,^3S_1$ atoms, which continue to be optically pumped during the afterglow.

The polarization of electrons extracted from the afterglow of a rather intense discharge at 0.11-torr pressure is shown in Fig. 8, as a function of time after termination of the discharge. The discharge was pulsed on for 50 $\mu$sec, and the extraction window of width 15 $\mu$sec was scanned over a 140-$\mu$sec afterglow period. The measured electron polarization is seen to rise from an initial value of 2%, characteristic of the active discharge, to an asymptotic value of about 17% in the late afterglow. This is consistent with the expected increase as a function of time in the ratio of electrons produced during the afterglow to residual electrons left over from the active discharge.

Figure 9 shows the electron polarization in the afterglow as a function of source-gas pressure. Each point in the figure represents the electron polarization averaged over the entire afterglow period so that the measured polarization is degraded by the electrons remaining from the active discharge. In all cases the discharge was active for 50 $\mu$sec followed by an afterglow period of 100 $\mu$sec. Most of the measurements were taken with a 2-mm $\times$2-mm exit canal, but data taken near the optimum pressure with a 1-mm$\times$1-mm exit canal are shown in the figure for comparison. At very high pressures (~ 1 torr) the polarization falls to about 1% which is equal to that measured in the active discharge at that pressure. This low value of polarization can be attributed to the $P$-state mixing process mentioned previously.

## VI. CONCLUSIONS

The following may be concluded from these investigations.

(i) The predominant source of ionization in weak electrical discharges in helium gas at pressures near 0.1 torr is metastable-metastable reactions

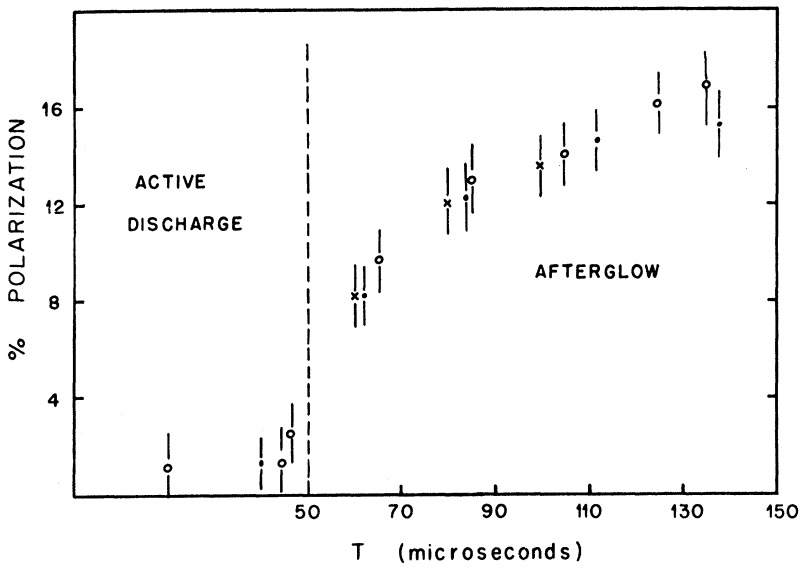


FIG. 8. Observed electron polarization vs time in the afterglow of a repetitively pulsed discharge. The gas pressure is 0.11 torr.

of the form $He^M + He^M \rightarrow He(1\,^1S_0) + He^+ + e^-$, where $He^M$ denotes a helium atom in either the $2\,^1S_0$ or the $2\,^3S_1$ metastable state.

(ii) The conclusion of the accompanying paper,[19] that spin angular momentum is conserved in metastable-metastable reactions, is independently confirmed.

(iii) An intense beam (several microamperes) of electrons with substantial spin polarization (8–10%) can be extracted from a helium discharge in which the $2\,^3S_1$ atoms are spin oriented by optical pumping. This polarized electron source would appear to be well suited for use in nuclear and atomic scattering experiments. It is capable of being operated in continuous or pulsed modes, the polarization direction can be easily reversed without affecting the beam trajectory, and it is inexpensive. Extracted electron polarizations as high as 17% have been realized in the late afterglow of a pulsed discharge, but only with a large sacrifice in beam current.

(iv) These results suggest the feasibility of measuring spin dependence of Penning reactions $He(2\,^3S_1) + X \rightarrow He(1\,^1S_0) + X^+ + e^-$, where $X$ is any molecule or atom other than neon, by means of an optically pumped flowing afterglow technique.[43] An improved polarized electron beam might be realized by judicious choice of $X$, since (a) the attainable $2\,^3S_1$ polarization is greater in the afterglow than in an active discharge, (b) every polarized metastable might be reacted to produce a polarized electron (in contrast to a conversion efficiency of

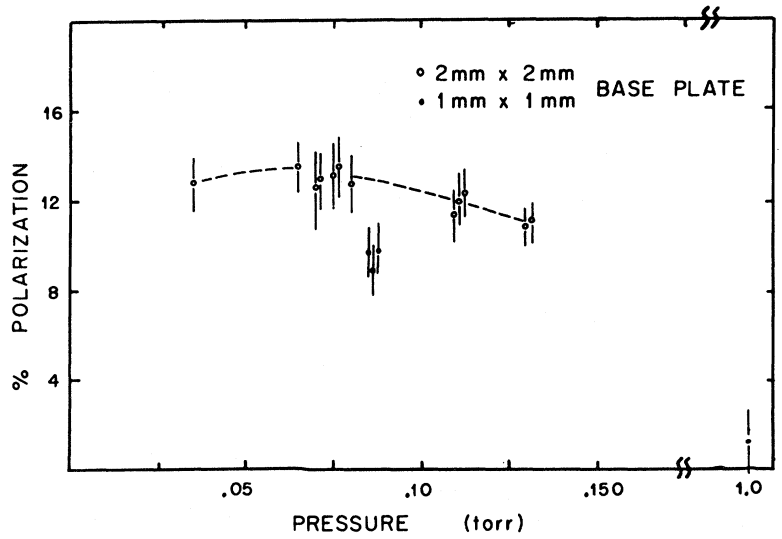


FIG. 9. Polarization of electrons extracted from the afterglow vs pressure. The polarization is averaged over the entire afterglow period (100 μsec).

no more than a few percent in the present experiments), and (c) the electrons can be thermalized prior to extraction by collisions with ground-state helium atoms, thus substantially narrowing the energy spread.


## ACKNOWLEDGMENTS

The authors gratefully acknowledge the help of Professor Joachim Kessler who directed us in the design and operation of the Mott scattering chamber and the electron optics system during his stay at Rice University. One of us (M. V. M.) wishes to thank the administrative staff of the Joint Institute For Laboratory Astrophysics, Boulder, Colorado, for secretarial and drafting services.


## APPENDIX: PARAMETERS $K$ AND $L$

The ratio $K:L:1$ characterizes the intensity of the $D_0$, $D_1$, and $D_2$ components of the $2\,^3S_1 - 2\,^3P_{0,1,2}$ pumping light relative to the corresponding absorption lines in the source gas. The uncertainty of this ratio arises from the fact that the emission lines from the lamp may be substantially shifted and broadened relative to the absorption lines. Estimates of $K$ and $L$ are based on the following limited information.

Schearer[42] has measured the relative shift between the absorption and emission lines for lamps and absorption cells similar to ours. His data suggest that the lines from the lamp are shifted by approximately $0.7 \pm 0.2$ cm$^{-1}$ toward lower energies.

Both Stockwell[44] and Schearer[21] have made high-resolution observations of the optical-pumping signal $\Delta I$; in their experiments the $\Delta I_0$ component was resolved from $\Delta I_1 + \Delta I_2$. The following relations can be inferred from the data:

$$\Delta I_0 \gg (\Delta I_1 + \Delta I_2)\,, \quad \Delta I_1 + \Delta I_2 \lesssim 0\,.$$

Using procedures similar to those outlined in Sec. II of this paper, each component of the optical signal may be written

$$\Delta I_0 = \tau F \tfrac{1}{3} K(5 + 9L + 8K) + (\tau F)^2 \tfrac{1}{2} K(1 + L)(5 + 9L + 8K)\,,$$

$$\Delta I_1 = \tau F L(5 + 9L + 2K) + \tfrac{3}{2}(\tau F)^2 L(1 + L)(5 + 9L + 8K)\,,$$

$$\Delta I_2 = -\tau F \tfrac{4}{3}(5 + 9L + 7K) - 2(\tau F)^2(1 + L)(5 + 9L + 8K)\,.$$

The values of $K:L:1$ which satisfy the experimental observations appear to be $K = 0.4 \pm 0.15$ and $L = 1.3 \pm 0.2$.

---

*Work supported in part by the U. S. Atomic Energy Commission. Based on a Ph. D. thesis by M. V. McCusker, Rice University, 1969.

†Present Address: Joint Institute for Laboratory Astrophysics, University of Colorado, Boulder, Colo. 80302.

‡Present Address: Physics Department, Texas Tech University, Lubbock, Tex. 79409.

[1]T. R. Holstein and I. B. Bernstein, Westinghouse Research Memo No. 60-94411-9-21, 1954 (unpublished); Phys. Rev. 94, 1475 (1954); A. D. MacDonald and S. C. Brown, Phys. Rev. 75, 111 (1949); G. Bekefi and S. C. Brown, J. Appl. Phys. 32, 25 (1961); R. Mewe, Rijnhuizen Report No. 69-50, Rijnhuizen, Jutphaas, Netherlands, 1969 (unpublished).

[2]See M. V. McCusker *et al.*, Phys. Rev. Letters 22, 817 (1969) for a preliminary report of this work.

[3]J. A. Hornbeck and J. P. Molnar, Phys. Rev. 84, 621 (1951); J. L. Franklin and F. A. Matsen, J. Chem. Phys. 41, 2948 (1964).

[4]F. D. Colegrove and P. A. Franken, Phys. Rev. 119, 680 (1960).

[5]L. D. Schearer, *Advances in Quantum Electronics* (Columbia U. P., New York, 1961), pp. 235–251.

[6]J. Kessler, Rev. Mod. Phys. 41, 3 (1969); W. Raith, *Atomic Physics* (Plenum, New York, 1969), pp. 389–415; P. S. Farago, Advan. Electron. Electron Phys. 21, 1 (1965).

[7]S. C. Brown, *Introduction to Electrical Discharges in Gases* (Wiley, New York, 1966), p. 165.

[8]T. R. Holstein and I. B. Bernstein, Ref. 1.

[9]D. Rapp and D. Englander-Golden, J. Chem. Phys. 43, 1464 (1965).

[10]D. R. Long and R. Geballe, Bull. Am. Phys. Soc. 11, 503 (1966).

[11]A. V. Phelps and J. P. Molnar, Phys. Rev. 89, 1202 (1953).

[12]A. C. G. Mitchell and M. W. Zemansky, *Resonance Radiation and Excited Atoms* (Cambridge U. P., Cambridge, England, 1961).

[13]R. Byerly, Ph. D. thesis (Rice University, 1967) (unpublished).

[14]E. W. McDaniel, *Collision Phenomena in Ionized Gases* (Wiley, New York, 1964).

[15]H. J. Oskam and V. R. Mittelstadt, Phys. Rev. 132, 1435 (1963).

[16]The use of an "effective" mobility here takes into account effects such as diffusion cooling in low-pressure helium diffusion.

[17]M. A. Biondi, Phys. Rev. 88, 660 (1952).

[18]However, the relative importance of direct ionization should increase with both discharge intensity (more high-energy electrons produced) and with gas pressure (increased frequency of electron-atom collisions). This is compatible with experimental observations that electron polarization decreases at high discharge intensities and gas densities (see Sec. IV).

[19]See J. C. Hill, L. L. Hatfield, N. D. Stockwell, and G. K. Walters, following paper, Phys. Rev. A 5, 189 (1972).

[20]A. V. Phelps, Phys. Rev. 99, 1307 (1955).

[21]L. D. Schearer, Phys. Rev. 160, 76 (1967).

[22]M. Fred, F. S. Tomkins, J. K. Brody, and M. Hammermesh, Phys. Rev. 82, 406 (1951).

[23]Conservation of spin angular momentum in the metastable-metastable reaction has been demonstrated directly by the experiments reported by Hill, Hatfield, Stockwell, and Walters, Ref. 19.

[24]R. F. Stebbings, Proc. Roy. Soc. (London) A241, 270 (1957).

[25]L. D. Schearer, Phys. Rev. 171, 81 (1968).

[26]The probability of spin exchange in the afterglow period may be somewhat greater than in an active discharge. However, the question is probably academic because there can be little doubt that the only electron-producing reaction in the afterglow ($He^M + He^M \rightarrow He + He^+ + e^-$) leaves the typical electron already spin polarized.

[27]J. A. Simpson and L. Marton, Rev. Sci. Instr. 32, 802 (1961); J. Kessler and H. Lindner, Z. Angew. Phys. 18, 7 (1964).

[28]The accelerating column and associated resistor chain were provided through the courtesy of Texas Nuclear Corp., Austin, Tex.

[29]H. A. Tolhoeck, Rev. Mod. Phys. 28, 277 (1956).

[30]N. F. Mott, Proc. Roy. Soc. (London) A124, 425 (1929).

[31]J. van Klinken, Nucl. Phys. 75, 163 (1966).

[32]L. Mikaelyan, A. Borovoi, and E. Denisov, Nucl. Phys. 47, 328 (1963).

[33]S. R. Lin, Phys. Rev. 133, A965 (1964).

[34]G. Holzworth and H. J. Meister, Nucl. Phys. 59, 56 (1968).

[35]K. Jost and J. Kessler, Z. Physik 195, 1 (1966); the plus sign in their paper is in error.

[36]J. Kessler (private communication).

[37]Pressure measurements are accurate to ±20%.

[38]The question of whether or not the collision of spin-oriented $2\,^3S_1$ metastables with a metal surface will produce a spin-polarized electron is being investigated in a separate experiment.

[39]W. A. Fitzsimmons, M. A. thesis (Rice University, 1966) (unpublished).

[40]P. A. Burke, in *Fifth International Conference on the Physics of Electronic and Atomic Collisions: Abstracts of Papers*, edited by I. P. Flaks (Nauka, Leningrad, 1967).

[41]The highest discharge intensity attainable at 0.035 torr with available excitation sources corresponded to 8% absorption of the pumping light.

[42]L. D. Schearer (private communication).

[43]An optical technique has been reported recently for measuring spin dependence of Penning reactions in which $X^+$ is produced in an electronically excited state. See L. D. Schearer, Phys. Rev. Letters 22, 629 (1969).

[44]N. D. Stockwell, Ph. D. thesis (Rice University, 1967) (unpublished).

PHYSICAL REVIEW A VOLUME 5, NUMBER 1 JANUARY 1972

# Direct Demonstration of Spin-Angular-Momentum Conservation in the Reaction $He(2\,^3S_1) + He(2\,^3S_1) \rightarrow He(1\,^1S_0) + He^+ + e^-$ †

J. C. Hill,* L. L. Hatfield, ‡ N. D. Stockwell, § and G. K. Walters
*Department of Physics, Rice University, Houston, Texas* 77001
(Received 21 June 1971)

Conservation of spin angular momentum in the reaction $He(2\,^3S_1) + He(2\,^3S_1) \rightarrow He(1\,^1S_0) \rightarrow He^+ + e^-$ is demonstrated quantitatively in the afterglow of a helium discharge by measuring the dependence of the electron production rate upon $2\,^3S_1$ spin-state populations, which are manipulated by an optical-pumping technique.

## I. INTRODUCTION

The combined use of microwave diagnostic techniques and optical pumping in $He^3$ has made possible a quantitative demonstration of the conservation of electron spin angular momentum in the reaction

$$He(2\,^3S_1) + He(2\,^3S_1) \rightarrow He(1\,^1S_0) + He^+ + e^- \qquad (1)$$

occurring in the afterglow of a pulsed helium discharge.

Violations of spin conservation in inelastic reactions involving $nF$ states of He are known to occur and are explained in terms of the failure of the $LS$ coupling approximation.[1] Nevertheless, in the preceding paper McCusker *et al.*[2] invoke spin-angular-momentum conservation to account for measured spin polarization of electrons produced by reaction (1) in $He^4$, and the present work independently confirms the validity of their assumption.

As a direct consequence of the conservation of spin angular momentum the cross section associated with Eq. (1) should depend in a predictable manner on the magnetic spin-states of the reactant $2\,^3S_1$ metastable atoms. Optical pumping is used to control the spin-state populations in the afterglow of a pulsed helium discharge, and microwave diagnostics are used to detect the corresponding change in the number density of electrons produced by the reaction. Since the various reactions in a helium afterglow are well understood, simple, and few in number, the resulting demonstration of spin-angular-momentum conservation is quite direct and unambiguous.

## II. THEORY OF EXPERIMENT

This experiment examines reactions occurring in room-temperature high-purity $He^3$ gas at a pressure of about 2 torr, in the afterglow periods following a repetitively pulsed electrical discharge. Upon termination of the discharge, all of the excited atoms present decay to the ground state within a time of the order of $10^{-7}$ sec, except for those